Am J Cancer Res 2023;13(11):5466-5481
www.ajcr.us /ISSN:2156-6976/ajcr0151040

Original Article

MIR-376A-2-5P as a potential prognostic marker for advanced penile squamous cell carcinomas trough HPV-dependent pathways

Jenilson M Silva[1,2], Amanda J Deus[1,2], André A M Vale[2,3], Ana Paula S Azevedo-Santos[3], Leudivan Nogueira[4], Ana C Laus[5], Luciane Sussuchi[5], Rui M Reis[5,6,7], Alexander Birbrair[8,9,10], André S Khayat[11,12], Silma Regina Pereira[2]

[1]Postgraduate Program in Health Science, Federal University of Maranhão, São Luís 65080-805, MA, Brazil; [2]Laboratory of Genetics and Molecular Biology, Department of Biology, Federal University of Maranhão, São Luís 65080-805, MA, Brazil; [3]Laboratory of Applied Cancer Immunology, Department of Physiological Sciences, Federal University of Maranhão, São Luís 65080-805, MA, Brazil; [4]Aldenora Bello Cancer Hospital, São Luís 65031-630, MA, Brazil; [5]Molecular Oncology Research Center, Barretos Cancer Hospital, Barretos 14784-400, SP, Brazil; [6]Institute for Research in Health and Life Sciences (ICVS), School of Medicine, University of Minho, Braga 4710-057, Portugal; [7]ICVS/3B's - PT Government Associate Laboratory, Braga/Guimarães 4710-057, Portugal; [8]Department of Pathology, Federal University of Minas Gerais, Belo Horizonte 31270-901, MG, Brazil; [9]Department of Dermatology, University of Wisconsin-Madison, Madison, WI 53715, USA; [10]Department of Radiology, Columbia University Medical Center, New York, NY 10032, USA; [11]Oncology Research Center, Federal University of Pará, Belém 66073-005, PA, Brazil; [12]Institute of Biological Sciences, Federal University of Pará, Belém 66077-830, PA, Brazil

Received May 3, 2023; Accepted August 16, 2023; Epub November 15, 2023; Published November 30, 2023

Abstract: Penile cancer (PeCa) is a rare tumor, generally associated with socioeconomic conditions in low-income countries. Hence, a delay in diagnosis and treatment leads in more advanced tumors, to higher comorbidity, and mortality. Human papillomavirus (HPV) infection has been identified as one of the major risk factors for PeCa. In addition, viral integration sites have been related to copy number alterations, impacting miRNAs/mRNA interactions and, consequently, the molecular pathways related to them. Nonetheless, studies on differentially expressed miRNAs (miRDEs) in PeCa are still scarce, especially in PeCa associated with high-risk HPV (hrHPV). To investigate the role of these gene regulators in PeCa progression, 827 miRNAs (Nanostring Technologies™, Seattle, WA, USA) were evaluated in 22 hrHPV-associated penile squamous cell carcinomas and five non-tumor penile tissues. For functions of miRNAs/target genes and relationship with HPV we conducted an integrated analysis by Diana Tools, KEGG, HPVbase, and InterSPPI-HVPPI platforms. We found that 25 miRNAs of the most differentially expressed impact 43 top molecular pathways, of which the fatty acid biosynthesis pathway, prions, miRNAs in cancer and hippo signaling ($P<1.0^{-325}$, for each) were the most statistically significant. Notably, 23 out of 25 are located at HPV integration sites (HPVis). MiR-1206, miR-376b-3p and miR-495-3p were downregulated and associated with perineural invasion. In addition, a comparison between advanced and early diseases revealed 143 miRDEs. ROC analysis of a single (miR-376a-2-5p), paired (miR-376a-2-5p, miR-551b-3p) or combination of five miRDEs (miR-99a-5p, miR-150-5p, miR-155-5p, let-7c-5p, miR-342-3p) showed robust discriminatory power (AUC = 0.9; P = 0.0114, for each). Strikingly, miR-376a-2-5p exhibited the highest values of sensitivity and specificity, with 100% and 83.3%, respectively, indicating this miRNA as a potential prognostic marker in hrHPV-penile carcinogenesis.

Keywords: HPV-integration sites, penile cancer, prognostic markers, miRNAs, perineural invasion

Introduction

Penile cancer (PeCa) is a rare neoplasm with a high incidence in low- and middle-income countries [1]. Brazil is among the countries with the highest incidence rates worldwide, with the Northeast region having the most significant number of cases [1, 2]. However, even in high-income countries, the incidence and mortality rates have increased in recent decades, especially in young men [3], which suggests that Human Papillomavirus (HPV) infection is possi-

bly the main factor for the development of penile tumors, in addition to other known risk factors, such as poor genital hygiene, phimosis, chronic inflammation, tobacco use and immunosuppression [1-3].

In clinical practice, cancer staging has been determined by clinical and histological characteristics, such as tumor grade, tumor stage, lymphovascular, lymph node, extranodal invasion, and lymph node metastases [4, 5]. In addition, perineural invasion (PNI) is a high-predictive-value risk factor for advanced PeCa, LNM, mortality, and survival (reviewed by Zhou et al. [6]). However, PNI did not gain prominence until the 8th TNM staging guideline (tumor, lymph node, and metastasis) was updated [5]. Consequently, there are limited data on the prognostic value of this pathological factor, especially regarding potential biomarkers associated with PNI in hrHPV-penile carcinogenesis.

Our previous studies have supported that hrHPV infection has a role in PSCC. In these studies, we described a high frequency of copy number alterations (CNAs) at HPV integration sites (HPVis) and the effect of microRNAs (miRNAs) on HPV-related molecular pathways [2, 7, 8]. Other authors have also associated miRNAs with penile carcinogenesis [9-14]; however, focusing on HPV-negative patients. Therefore, it is important to investigate the involvement of miRNAs in advanced hrHPV-associated PSCC. Hence, considering the role of HPV infection in the classification of PeCa [15], and the high frequency of hrHPV-associated advanced PSCC in Northeast Brazil, we explored the role of miRNAs differentially expressed (miRDEs) in the PSCC, as potential prognostic markers. Further, we investigated molecular pathways potentially impacted by miRDEs that may help to clarify the mechanisms underlying the development of PSCC, which may serve as a basis for future therapeutic strategies.

Materials and methods

Study population

Twenty-two PeCa samples and five non-tumor adjacent penile tissues (2 cm distant from the tumor) are a subset of samples obtained at the Aldenora Bello Cancer Hospital, São Luís, Maranhão, Brazil, from 2013 to 2016 [2]. All patients admitted to the study signed written Informed Consent, which was approved by the Research Ethics Committee on Humans from the Federal University of Maranhão and by the National Research Ethics Commission (CONEP, Brazil; CAAE: 46371515.5.0000.5087). Only patients aged >18 years, with a clinical and anatomopathological diagnosis of penile cancer, participated in the study. All tissues were obtained at the time of surgery and before any cancer treatment. Patients who did not fit these criteria and or did not agree to sign the Informed Consent were excluded from the study. Clinical and histopathological data were obtained from the patients' medical records.

The mean age at diagnosis was 64.2 ± 15.6, ranging from 32 to 85 years old. Most patients were married (77.3%) and had a low education level; 18.1% had completed high school. All tumors were classified as Squamous Cell Carcinoma (SCC), with a mean size of 4.4 ± 2.4 cm, ranging from 0.8 to 10 cm. Phimosis was observed in 36.4% of patients, the majority being over 40 years old (87.5%). The clinical and histopathological data of the patients are presented in **Table 1** and Supplementary Table 1.

HPV genotyping

All patients were positive for HPV, as described by Macedo et al. [2]. Briefly, HPV genotyping was performed by nested-PCR (according to BioGenetics Molecular Technologies, Uberlândia, Minas Gerais, Brazil; patent number BR102017004615.0) and by DNA sequencing. In 94.4% of patients, high-risk HPV was detected, with subtype HPV16 being the most frequent (72.2%), followed by HPV74 (16.6%), HPV30, HPV59, and HPV66 (11% each). Multiple infections were detected in 50% of the cases (Supplementary Table 1).

miRNAs differential expression analysis

We analyzed the global differentially expressed miRNAs from 22 PSCC and five adjacent non-tumor tissues [data available in *The Gene Expression Omnibus* (GEO), under registration GSE197121] as cited by da Silva et al. [8] (Supplementary Table 2). Briefly, RNA was isolated using the TRIzol protocol (Invitrogen, Walthan, MA, USA). RNA concentration and quality control were verified by measuring the

Table 1. Clinical-histopathological variables of patients with HPV-positive penile squamous cell carcinoma (n = 22)

Characteristic	Number (%)	Characteristic	Number (%)
Stage (pT)		Lesion characteristic	
pT1	6 (27.3%)	Ulcerated	9 (41%)
pT2	9 (40.9%)	Vegetative	4 (18.2%)
pT3	7 (31.8%)	Verrucous	3 (13.6%)
Grade (Gx)		Nodular ulcerated	3 (13.6%)
G1	4 (18.2%)	Ulcer-vegetative	3 (13.6%)
G2	12 (54.5%)	Anatomical site of the tumor	
G3	6 (27.3%)	Glans	9 (40.9%)
Lymphatic invasion		Glans and foreskin	7 (31.8%)
Positive	4 (18.2%)	Foreskin	2 (9.1%)
Negative	17 (77.3%)	Glans, foreskin, and other areas	4 (18.2%)
No information	1 (4.5%)	Type of surgery	
Perineural invasion		Partial penectomy	17 (77.3%)
Positive	5 (22.8%)	Total penectomy	5 (22.7%)
Negative	16 (72.7%)	Phimosis	
No information	1 (4.5%)	Yes	8 (36.4%)
Tumor size (cm)		No	9 (40.9%)
0.6-2.0	4 (18.2%)	No information	5 (22.7%)
2.1-5.0	15 (68.2%)	Smoking	
5.1-10.0	3 (13.6%)	Yes	9 (41.0%)
Histological type		No	10 (45.4%)
Usual	8 (36.4%)	No information	3 (13.6%)
Condylomatous	10 (45.4%)	Alcoholism	
Usual and basaloid	2 (9.1%)	Yes	10 (45.4%)
Usual and condylomatous	2 (9.1%)	No	7 (31.9%)
			No information

260/280 and 260/230 ratios (Nanodrop 2001 spectrophotometer; Willington, DE, USA). MiRNA expression was evaluated using the nCounter® Human v.3 miRNA Expression platform (Nanostring Technologies™, Seattle, WA, USA), according to the manufacturer protocol. We performed two miRNAs differential expression analyses: (i) between 22 tumors and five non-tumor tissues; and (ii) between 5 tumors paired with their respective non-tumor tissues (Supplementary Figure 1). Raw data were normalized using the ROSALIND® Nanostring platform (https://rosalind.onramp.bio/). Distribution percentages, heatmaps and other graphs were generated as part of the QC step. Normalization was performed following background subtraction based on the correction factors of the POS_A probes (positive control normalization and codeset normalization). For both steps, the geometric mean of each set of probes was used to create a normalization factor. Fold Change (≥2 and ≤-2) and *p*-values for comparisons were calculated using the t-test (P≤0.05). The *p*-value adjustment (adj.-*p*) was performed using the Benjamini-Hochberg method (P≤0.01) to estimate false discovery rates (FDR). The clustering of miRNAs for the heatmap was constructed using PAM (*Partitioning Around Medoids*) through a method using the FPC-R library [16] that considers the pathways, functions, and types of each identified miRNA.

To identify a panel of miRNAs that could distinguish advanced disease from early disease, tumor samples were stratified based on two clinical groups: (i) advanced disease, consisting of tumors with positive perineural invasion and pT3 staging (5 samples); (ii) early disease, consisting of tumors with negative perineural invasion and pT1 or pT2 staging (12 samples). The data were analyzed using the same criteria as described above.

Integrative analysis of miRDEs across tumor types

To identify specific miRDEs in PSCC, the miRNA expression data of different cancers, including squamous cell carcinomas and HPV-related, were compared to those of PSCC. Head and neck squamous cell carcinoma (HNSC) RNA-seq data were obtained from The Cancer Genome Atlas (TCGA, Firehose Legacy), which contains 497 tumors and 44 normal tissues. In addition, we compared 749 samples from 18 types of cancer (breast, endometrial, ovarian, gastroesophageal, head and neck, melanoma, hepatobiliary, non-small cell lung, bladder, lung, colorectal, uterine endometrium, cervix, renal, sarcoma, prostate, thyroid cancer, and glioma) from the Pan-cancer Analysis of Whole Genomes project (The ICGC/TCGA Pan-Cancer Analysis of Whole Genomes Consortium, 2020) [accessed cBioPortal [17, 18] (https://www.cbioportal.org/; on 25 Apr 2022)]. The HNSC-TCGA data were accessed through the ENCORI platforms [19] (https://starbase.sysu.edu.cn/index.php; accessed on January 28, 2022) and UALCAN [20] (http://ualcan.path.uab.edu/index.html; accessed January 28, 2022). Tumor and normal samples were statistically compared by t-test ($P \leq 0.05$) with z-scores log FPKM relative to all samples, and by type of cancer with z-scores UQ normalized, as log2(value + 1).

Association of miRDEs with patients' clinical and histopathological characteristics

The normality of each miRNA's relative expression was assessed using the Shapiro-Wilk test. If the data presented a normal distribution, the t-test was employed to compare two groups; otherwise, the Mann-Whitney test was utilized. To compare three or more clinical parameters, a one-way ANOVA with Tukey's post hoc was conducted on normally distributed data; if not, the Kruskal-Wallis test with Dunn's correction was employed. The significance level was $P \leq 0.05$ and adj.-$P \leq 0.01$. Statistical tests were performed using GraphPad Prism v.9 software.

Receiver operating characteristic (ROC) curve analysis

ROC curve analysis and Area Under the Curve (AUC) determination were performed to validate the ability of miRDEs to discriminate between advanced and early diseases. Sensitivity and specificity were computed using the normalized expression data. An AUC of 100% denotes perfect miRDEs discrimination, whereas an AUC of 50% indicates poor discrimination. For each miRDE, AUCs and 95% confidence intervals (CI) were determined. Moreover, a significance level of $P \leq 0.05$ was employed with the Wilson/Brown method correction. Additionally, the miRDEs with the highest AUC were combined to create a robust panel for discriminating clinical groups. The panels with the greatest AUC values on ROC curves were chosen to calculate the Youden Index (J) in order to determine the point with the most sensitivity and specificity. Statistical tests were performed using GraphPad Prism v.9 software.

Target genes and pathway enrichment analysis

The DIANA-Tarbase v.8 [21] and miRTarBase [22] databases were used to determine interactions among miRDEs and validated target genes based on miTG (miRNA Target Gene) ≥ 0.8; robust experimental (luciferase reporter assay, western blot, and qPCR) and less robust (microarray, NGS and pSilac) assays. DianamiRPath v.3.0 [23] was used to identify the signaling pathways affected by miRDEs, using the Kyoto Encyclopedia of Genes and Genomes (KEGG) platform. The target genes were predicted by micro-TCDS algorithms (v.5) with $P < 0.05$, microT of 0.8 and miTG≥ 0.8. The top pathways were identified using the "pathways union" function.

Protein-protein interactions (PPI) based on miRDEs target genes and HPV oncoproteins

We investigated interactions among human proteins encoded by miRDE target genes. For this, we used I2D [24], STRING v.11 [25], and BioGRID v.4.4 [26], with a minimum interaction score of 0.9 (high confidence). HPV integration sites in human cytobands were identified by accessing the HPVbase databases [27] (http://crdd.osdd.net/servers/hpvbase/index.html) (accessed on April 12, 2022) and VISDB [28] (https://bioinfo.uth.edu/visdb/index.php/homepage) (accessed on April 12, 2022).

We applied InterSPPI-HVPPI (http://zzdlab.com/hvppi/; accessed on December 24, 2021) in accordance with Yang et al. [29] to evaluate interactions between protein-HPV and protein-human using a machine learning method based on amino acid sequences obtained from the

KEGG platform's genes. Due to the prevalence of HPV16 in our samples, the E5, E6, and E7 proteins from this subtype (id: P06927, id: P03126, and id: P03129, respectively) were utilized for prediction analysis. Interactions between miRNAs, genes, and potential drug targets were predicted by Drug Gene Interaction Database v.4.2 (DGIdb) according to Freshour et al. [30]. Cytoscape v.3.8.2 and PathVisio v.3.3 were utilized to accomplish pathway enrichment.

Results

miRDEs in hrHPV-associated PSCC

First, to validate the normal control group (n = 5), the expression pattern of 22 tumors *versus* 5 non-tumor tissues was compared with the expression pattern of the paired group (5 tumors and their respective non-tumor tissues) (Supplementary Figure 1). In addition to the 13 miRDEs described by da Silva et al. [8] as being upregulated (let-7a-5p, miR-130a-3p, miR-142-3p, miR-15b-5p, miR-16-5p, miR-200c-3p, miR-205-5p, miR-21-5p, miR-223-3p, miR-22-3p, miR-25-3p, miR-31-5p, and miR-93-5p), we selected 12 miRDEs with the lowest expression levels (cutoff point Log2FC≤-2.9): miR-1206, miR-144-3p, miR-190b, miR-376b-3p, miR-381-5p, miR-433-3p, miR-495-3p, miR-508-3p, miR-509-3-5p, miR-509-3p, miR-544a, and miR-661, totaling 25 miRDEs. Interestingly, 92% (n = 23/25) of these miRDEs are within HPVis, with HPV16 being the most frequent subtype. The 25 miRDEs were used for all comparisons with TCGA miRNA expression data, as well as for target prediction and pathway enrichment. **Figure 1A** and **Table 2** list the top 25 miRDEs related to hrHPV-associated PSCC.

Cross-study with TCGA-data

We compared the top 25 PSCC-miRDEs with HNSC-miRDEs (**Table 2**). The majority of miRDEs in PSCC (80%, n = 20/25) exhibited the same *status* in HNSC. We emphasize that miR-1206, miR-544a, and miR-661, downregulated in PSCC, did not have changes in their expression in HNSC. To investigate the expression of these miRNAs in other cancers, we performed a comparative analysis with expression data from 749 samples of 18 types of cancers from the "Pan-cancer Analysis of Whole Genomes" project (ICGC/TCGA). MiR-544a was upregulated only in glioblastoma, whereas miR-661 and miR-1206 were not differentially expressed in any of the 18 cancers evaluated.

MiRDEs and their association with clinical and histopathological parameters

The analysis of the 25 miRDEs with the clinical and histopathological parameters revealed an association between the downregulation of miR-1206 (P = 0.0044), miR-376b-3p (P = 0.0392) and miR-495-3p (P = 0.0341) and perineural invasion. In addition, overexpression of let-7a-5p (P = 0.05), miR-200c-3p (P = 0.05), and miR-205-5p (P = 0.01) was associated with tumor grade, presenting a difference between intermediate and advanced grade tumors (adj.-*P* = 0.05, 0.0459 and 0.0073, respectively). Additionally, miR-142-3p was associated with tumor staging (P = 0.0126), with differential expression between early and intermediate staging (pT1 *vs.* pT2, adj.-*P* = 0.0257) and between intermediate and advanced tumors (pT2 *vs.* pT3, adj.-*P* = 0.0329). See **Table 3**.

In silico functional analysis and miRNA/mRNA interaction networks

The potential biological impact of miRDEs was predicted from experimentally validated interactions between miRNAs and their target genes. Of the top 25 miRDEs, only miR-1206 had no validated targets. The 24 miRDEs regulate 2,284 genes in 3,419 interactions (Supplementary Table 3A). miR-661, miR-16-5p, and miR-15b-5p had the highest number of targets (459, 438, and 395, respectively). On the other hand, miR-376b-3p, miR-495-3p, and miR-509-5p had the lowest number of targets (2, 2, and 3, respectively). We identified 43 KEGG pathways (Supplementary Table 3B), of which the top 15 are related to cancer (P≤0.00017): fatty acid biosynthesis (hsa-00061), prion diseases (hsa05020), cancer microRNAs (hsa05206), hippo signaling pathway (hsa04390), TGF-beta signaling pathway (hsa04350), oocyte meiosis (hsa04114), lysine degradation (hsa00310), glioma (hsa05214), foxO signaling pathway (hsa04068), signaling pathways that regulate stem cell pluripotency (hsa04550), prostate cancer (hsa05215), cancer proteoglycans (hsa05205), p53 signaling pathway (hsa04115), mTOR signaling pathway (hsa04150) and fatty acid metabolism (hsa01212). All top pathways identified are

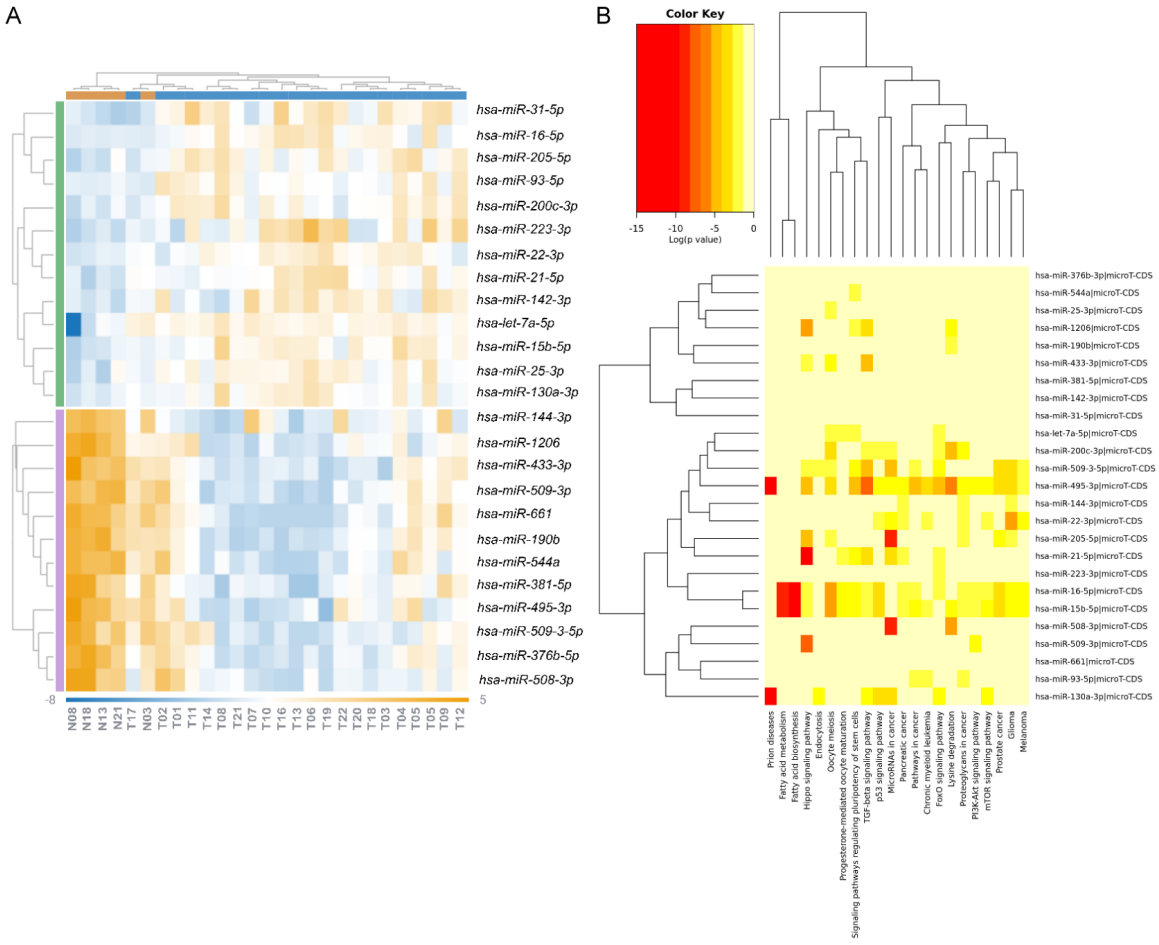

Figure 1. Unsupervised hierarchical clustering of the 25 miRDEs and related top pathways. A. The heatmap generated by miRNA expression patterns showed two distinct groups (upper cluster) formed by tumor samples (blue bar) and normal samples (orange bar). The hierarchical group on the left is formed by miRNAs upregulated (green bar) and downregulated (pink bar). On the heatmap, orange colors indicate upregulated miRNAs, and blue colors indicate downregulated miRNAs. B. The heatmap shows a compilation of the top pathways identified by the prediction method (microT-CDS - pathways union). On the right, the 25 miRDE and the target prediction algorithm used. Below is a compilation of the top pathways identified. Yellow colors indicate low impact of miRNAs on pathways, and orange and red colors indicate medium and high impact, respectively.

shown in **Figure 1B** and Supplementary Table 3C.

The enrichment pathways analysis revealed two distinct clusters (**Figure 1B**). The largest cluster comprises 16 miRDEs, most of which are upregulated. This cluster had the most significant impact on the top identified pathways. The second larger cluster comprises six downregulated and three upregulated miRDEs with a low impact on the top identified pathways. Furthermore, miR-200c-3p and let-7a-5p related to tumor grade, and miR-16-5p and miR-15-5p related to tumor lesions were identified, forming highly related clusters. In addition to the top pathways, we identified twelve genes regulated by miRDEs that had not yet been described in PSCC. **Table 4** shows the twelve target genes regulated by miRDEs in hrHPV-associated PSCC.

Human-proteins and HPV-oncoproteins interactions and druggable targets

Docking by sequence incorporation between human-protein and HPV-oncoprotein was performed using twelve predicted genes shown in **Table 4**. E7 oncoprotein strongly interacts with DDX3X (score = 0.758) and HSPA1B (score = 0.6) and moderately interacts with CHMP2B (score = 0.506), PTEN (score = 0.470), IKBKB

Table 2. The top 25 microRNAs differentially expressed in high-risk HPV-associated penile squamous cell carcinoma compared to head and neck squamous cell carcinoma

miRNAs	PSCC (this study) (22 tumors and 5 non-tumors)							HNSC (TCGA) (497 tumors and 44 normal)			
	Cytoband	Start-End (pb)	HPVis (genotype)*	MiRNA Expression	Log2FC	*p-value*	Adj.-*p*	MiRNA Expression	Log2FC	*p-value*	Adj.-*p*
let-7a-5p	9q22.32	96,938,234-96,938,325	yes, (16, 18)	Upregulated	2.2266	0.0019	0.0044	Downregulated	0.79	<0.0001	0.0003
miR-130a-3p	11q12.1	57,641,198-57,641,286	yes, (16)	Upregulated	1.1603	0.0008	0.0024	Upregulated	1.86	<0.0001	<0.0001
miR-142-3p	17q22	58,331,222-58,331,327	yes, (16)	Upregulated	1.4576	0.0054	0.0089	Upregulated	2.30	<0.0001	<0.0001
miR-15b-5p	3q25.33	160,404,588-160,404,685	yes, (16)	Upregulated	1.6509	<0.0001	0.0006	Upregulated	1.96	<0.0001	<0.0001
miR-16-5p	13q14.2	50,623,109-50,623,197	yes, (16)	Upregulated	1.2512	0.0008	0.0024	Upregulated	1.60	<0.0001	<0.0001
miR-200c-3p	12p13.31	6,963,694-6,963,771	no	Upregulated	1.2541	0.0023	0.0049	Upregulated	1.51	<0.0001	0.0013
miR-205-5p	1q32.2	209,428,820-209,432,384	yes, (16, 18)	Upregulated	1.4610	0.0013	0.0035	Upregulated	2.35	<0.0001	<0.0001
miR-21-5p	17q23.1	59,841,262-59,841,342	yes, (16, 18)	Upregulated	1.4629	0.0004	0.0016	Upregulated	2.67	<0.0001	<0.0001
miR-223-3p	Xq12	66,018,870-66,018,979	no	Upregulated	2.0222	0.0028	0.0056	Upregulated	1.26	0.059	0.17
miR-22-3p	17p13.3	1,617,197-1,617,281	yes, (16, 18)	Upregulated	1.0605	0.0018	0.0043	Upregulated	0.93	0.047	0.83
miR-25-3p	7q22.1	100,093,560-100,093,643	yes, (16)	Upregulated	1.5448	0.0001	0.0008	Upregulated	1.79	<0.0001	<0.0001
miR-31-5p	9p21.3	21,512,113-21,512,191	yes, (18)	Upregulated	2.0012	0.0006	0.0020	Upregulated	6.15	<0.0001	<0.0001
miR-93-5p	7q22.1	99,691,391-99,691,470	yes, (16)	Upregulated	1.0525	0.0016	0.0040	Upregulated	2.79	<0.0001	<0.0001
miR-1206	8q24.21	129,021,144-129,021,202	yes, (16, 18, 45)	Downregulated	-3.0310	<0.0001	0.0005	IE	1.07	0.77	0.82
miR-144-3p	17q11.2	27,188,551-27,188,636	yes, (16)	Downregulated	-2.9494	<0.0001	0.0006	Downregulated	0.37	<0.0001	<0.0001
miR-190b	1q21.3	154,193,662-154,193,747	yes, (16, 18)	Downregulated	-3.0044	<0.0001	0.0006	Downregulated	0.49	0.015	0.0550
miR-376b-3p	14q32.31	101,040,436-101,040,535	yes, (16)	Downregulated	-2.9871	<0.0001	0.0005	Downregulated	0.74	0.0081	0.033
miR-381-5p	14q32.31	101,045,918-101,045,996	yes, (16)	Downregulated	-2.9859	<0.0001	0.0006	Downregulated	0.18	<0.0001	0.0002
miR-433-3p	14q32.2	100,881,886-100,881,978	yes, (16)	Downregulated	-2.9974	<0.0001	0.0006	Downregulated	0.45	<0.0001	<0.0001
miR-495-3p	14q32.31	101,033,755-101,033,836	yes, (16)	Downregulated	-3.1037	<0.0001	0.0007	Downregulated	0.36	<0.0001	<0.0001
miR-508-3p	Xq27.3	146,318,431-146,318,545	yes, (16)	Downregulated	-2.9449	<0.0001	0.0006	Downregulated	1.80	<0.0001	0.0045
miR-509-3-5p	Xq27.3	146,341,170-146,341,244	yes, (16)	Downregulated	-2.9414	<0.0001	0.0006	Downregulated	0.34	<0.0001	0.0025
miR-509-3p	Xq27.3	147,260,532-147,260,625	yes, (16)	Downregulated	-3.0481	<0.0001	0.0006	Upregulated	4.15	0.097	0.26
miR-544a	14q32.31	101,048,658-101,048,748	yes, (16)	Downregulated	-3.0781	<0.0001	0.0006	IE	1.01	0.58	0.82
miR-661	8q24.3	145,019,359-145,019,447	yes, (16, 18)	Downregulated	-3.1792	<0.0001	0.0006	IE	1.26	0.55	0.82

*Data obtained from HPVBase [27] (accessed on April 12, 2022) and VISDB [28] we systematically collected and manually curated all VISs reported in the literature and publicly available data resources to construct the Viral Integration Site DataBase (VISDB), https://bioinfo.uth.edu/VISDB (https://bioinfo.uth.edu/VISDB/index.php/homepage) (accessed on Apr 12, 2022); miRNAs = microRNAs; IE = Insignificant expression; PSCC = Penile Squamous Cell Carcinomas; HPVis = Human Papilloma Virus Integration Site; HNSC = Head Neck Squamous Cell Carcinoma; TCGA = The Cancer Genome Atlas.

Table 3. Differentially expressed microRNAs in association with clinical and histopathological parameters in patients with HPV-positive penile squamous cell carcinoma

miRDE	miRNA Expression	Variables	*p-value*	Group (*p-value*)
let-7a-5p	Upregulated	Grade	0.05	G2 *vs.* G3 (0.05)
miR-200c-3p	Upregulated	Grade	0.05	G2 *vs.* G3 (0.0459)
miR-205-5p	Upregulated	Grade	0.0100	G2 *vs.* G3 (0.0073)
miR-142-3p	Upregulated	Staging	0.0126	pT1 *vs.* pT2 (0.0257) pT2 *vs.* pT3 (0.0329)
miR-144-3p	Downregulated	Staging	0.0197	pT1 *vs.* pT2 (0.0199)
miR-15b-5p	Upregulated	Size	0.0192	2.1-5 *vs.* 5.1-10 (0.0190)
		Lesion	0.0191	Ulcerated *vs.* vegetative (0.0371) Vegetative *vs.* verrucous (0.0353)
miR-16-5p	Upregulated	Lesion	0.0202	Ulcerated *vs.* vegetative (0.0395)
miR-25-3p	Upregulated	Lesion	0.0386	Ulcerated *vs.* vegetative (0.0304)
		Size	0.0007	0.6-2 *vs.* 2.1-5 (0.0005) 0.6-2 *vs.* 5.1-10 (0.0160)
miR-93-5p	Upregulated	Size	0.0286	0.6-2 *vs.* 2.1-5 (0.0221)
miR-130a-3p	Upregulated	Lesion	0.0154	Ulcerated *vs.* vegetative (0.0111)

miRDE = microRNAs differentially expressed.

Table 4. New target genes potentially regulated by microRNAs differentially expressed in HPV-positive penile squamous cell carcinoma

Gene	miRDE	miRNA Expression	miTG	*p-value*	Biological consequence
MDM2	*miR-661*	Downregulated	0.800	0.001	Ubiquitination and degradation of p53
MDM4	miR-433-3p	Downregulated	0.800	0.001	Ubiquitination and degradation of p53
	miR-661	Downregulated	0.800	0.001	
LDLR	miR-130a-3p	Upregulated	0.960	0.001	Deregulation of cholesterol metabolism
HSPA1B	miR-142-3p	Upregulated	0.802	0.001	Protein instability
VPS37C	miR-15b-5p	Upregulated	0.850	0.001	ESCRT-I (endosomal sorting complex required for transport I) dysregulation
	miR-16-5p	Upregulated	0.859	0.001	
CHMP2B	miR-200c-3p	Upregulated	0.812	0.001	ESCRT-III (endosomal sorting complex required for transport III) dysregulation
DDX3X	miR-15b-5p	Upregulated	0.992	0.002	Loss of expression induces resistance to chemotherapy, while its expression is related to viral replication
	miR-16-5p	Upregulated	0.993		
	miR-25-3p	Upregulated	0.869		
	miR-495-3p	Downregulated	1.000		
PTEN	miR-22-3p	Upregulated	0.911	0.002	Inhibition of apoptosis and induction of cell proliferation and growth
	miR-205-5p	Upregulated	0.937		
	miR-130a-3p	Upregulated	0.861		
IKBKB	miR-15b-5p	Upregulated	0.861	0.008	Inhibition of apoptosis and increased cell survival
	miR-16-5p	Upregulated	0.892		
PRDM4	miR-15b-5p	Upregulated	1.000	0.008	Cell cycle progression, activation of PI3K/AKT signaling and *PTEN* inhibition
	miR-16-5p	Upregulated	1.000		
WASL	mir-130a-3p	Upregulated	0.919	0.007	Destabilization of the cytoskeleton
MET	miR-144-3p	Downregulated	0.800	0.007	Increased cell survival and induction of cell migration and invasion.
	miR-433-3p	Downregulated	0.800	0.007	

miRDE = microRNA Differentially Expressed; miTG = microRNA Target Gene; hrHPV = high-risk Human Papilloma Virus.

(score = 0.455), WASL (score = 0.433) and PRDMD4 (score = 0.429) proteins. E5 and E6 interact with HSPA1A (score = 0.461 for E5, score = 0.415 for E6) and DDX3X

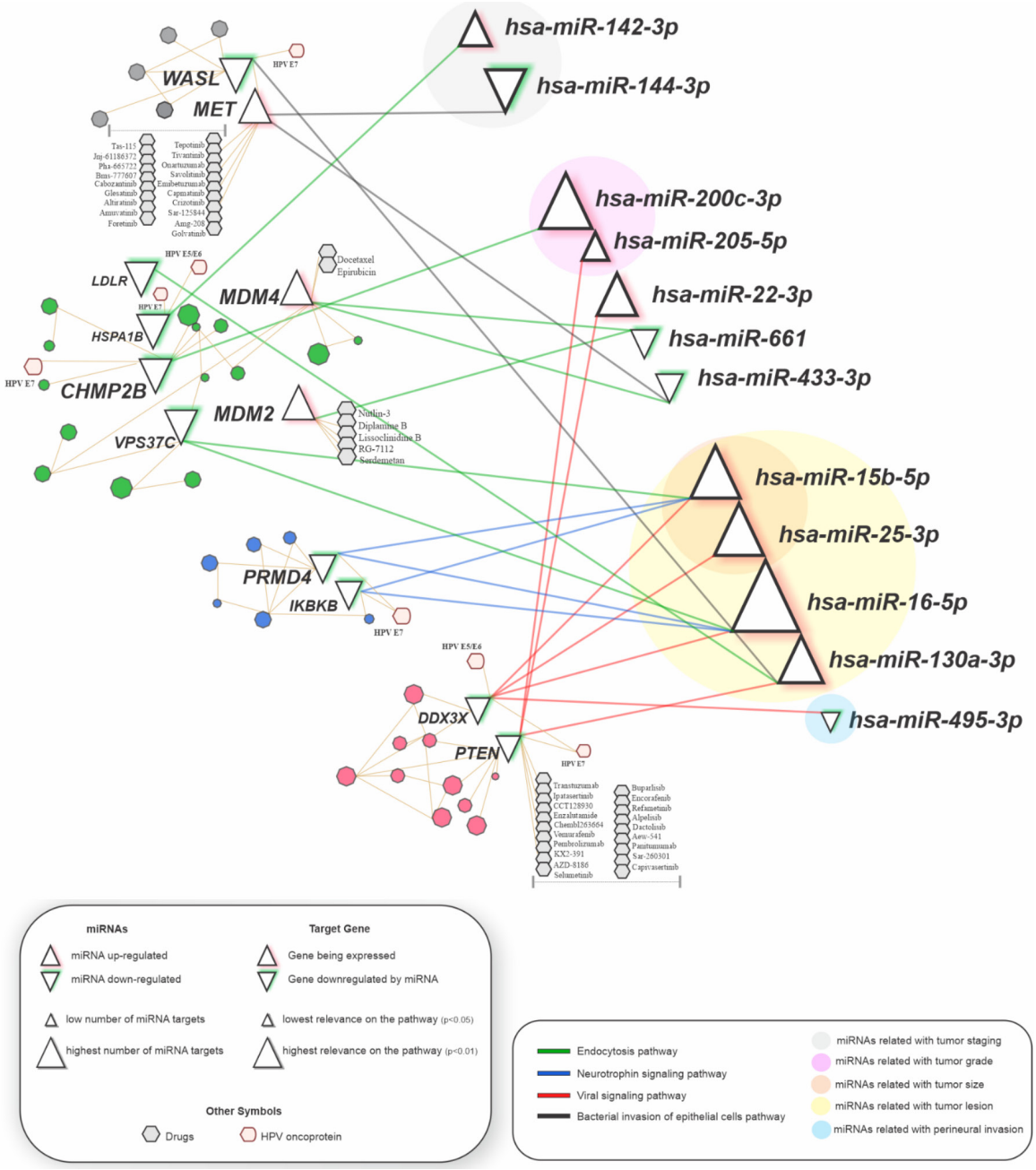

Figure 2. An integrative network between miRDEs and targets genes, HPV oncoproteins, and the predicted drugs. The significance of symbols and colors is shown in the tables below the integrative network. The network was generated by Cytoscape v.3.8.2 and PathVisio v3.3 software.

(score = 0.408 for E5, score = 0.566 for E6) proteins.

The drug prediction analysis, based on twelve genes and their miRDEs (**Table 4**), revealed five MDM2 inhibitors (nutlin-3; diplamine B; lissoclinidine B, RG-7112 and serdemetan), two drugs (epirubicin and docetaxel) targeting the MDM4 pathway, and nineteen drugs targeting the PTEN-PI3K/AKT and MET signaling pathways (**Figure 2**).

miRDEs as potential prognostic marker in PSCC

The stratification of PSCC patients into two clinical groups, (i) advanced disease and (ii) early disease, revealed 143 miRDEs, of which 5 (3.5%) are upregulated and 138 (96.5%) are

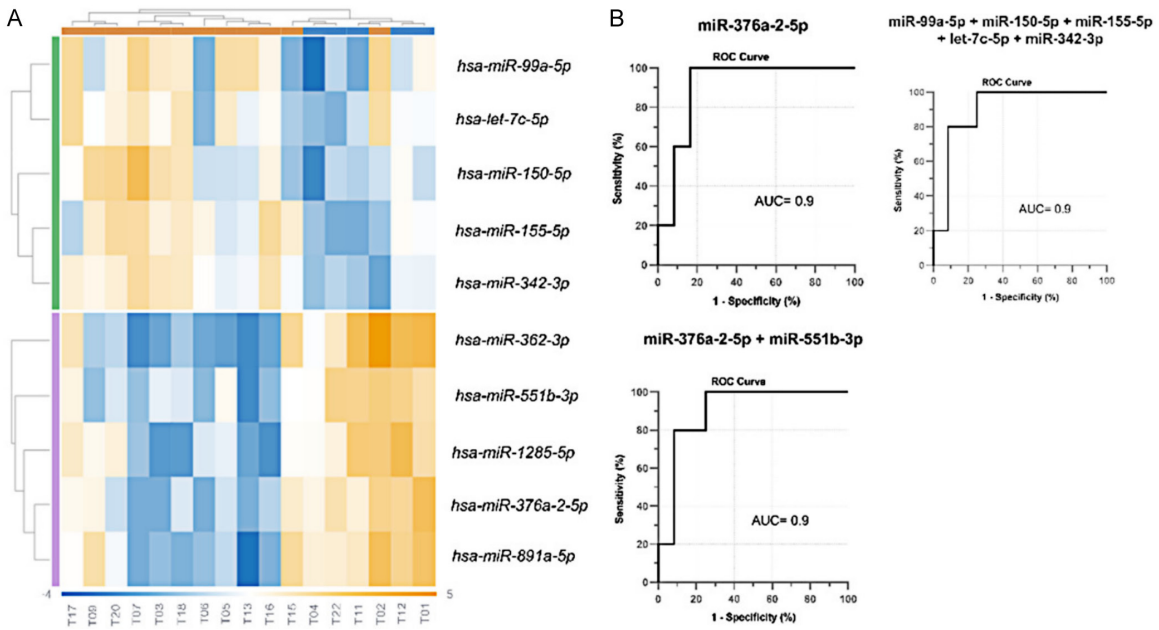

Figure 3. Unsupervised hierarchical clustering of the ten miRDEs with ROC curve analysis in hrHPV-associated PSCC. A. The heatmap generated by miRNA expression patterns showed two distinct groups (upper cluster) formed by advancing tumor samples (blue bar) and early tumor samples (orange bar). The hierarchical group on the left is formed by the upregulated (green bar) and downregulated (pink bar) miRNAs. On the heatmap, orange colors indicate upregulated miRNAs, and blue colors indicate downregulated miRNAs. B. ROC curve analysis shows AUC equal to 0.9. In each of the three graphs, the *p-value* was equal to 0.0114.

downregulated in advanced disease (Supplementary Table 4). Interestingly, the 5 upregulated miRNAs (miR-99a-5p, miR-150-5p, miR-155-5p, let-7c-5p, miR-342-3p) and the 5 most downregulated (miR-891a-5p, miR-376a-2-5p, miR-551b-3p, miR-1285-5p and miR-362-3p; cutoff point FC≤-1.8 and *p*-value ≤0.05), are all within HPVis. The top 10 miRDEs that distinguish individuals with advanced disease from those with early disease are displayed in **Figure 3A** and **Table 5**.

The PSCC staging analysis revealed AUC values over 0.8. We performed several combinatorial analyses between miRDEs to identify the most robust panel (Supplementary Figure 2). Two panels [1. combining the five most upregulated miRNAs (miR-99a-5p + miR-150-5p + miR-155-5p + let-7c-5p + miR-342-3p), and 2. combining the two most downregulated miRNAs (miR-376a-2-5p + miR-551b-3p)] exhibited discriminating power with an AUC value of 0.9 (P = 0.0114; 95% CI = 0.7475 to 1.000) (**Figure 3B**), with 100% sensitivity and 75% specificity, respectively, for each. We highlight that miR-376a-2-5p had an AUC of 0.9 (P = 0.0114; 95% CI = 0.7483 to 1.000), with a sensitivity of 100% and a specificity of 83.3% (95% CI = 0.7483 to 1.000).

We also compared the ten PSCC-miRDE with HNSC-miRDE and *Pan-Cancer* (ICGC/TCGA) (**Table 5**). Among ten PSCC-miRDE, five of them behave similarly in HNSC. A comparative analysis between the 10 PSCC-miRDEs and *Pan-cancer* data demonstrated that the expression of these miRNAs varied among the 18 analyzed cancer types.

Discussion

In this study, miRDEs between hrHPV-positive penile tumors and adjacent non-tumors tissues were investigated by expression matrix analysis. Our panel showed that 507 miRNAs are differentially expressed at statistically significant levels in hrHPV-positive tumors in relation to non-tumors tissue. The majority of miRDEs (97.4%) identified were downregulated. Our findings corroborate Ayoubian et al. [9], who identified a panel of miRNAs in HPV-positive penile tumors where 99.1% were downregulated. A large number of downregulated miRNAs may be mainly related to the activity of HPV E6

Table 5. Top 10 microRNAs differentially expressed between advanced and early clinical groups in high-risk HPV-associated penile squamous cell carcinoma and microRNAs differentially expressed described for head and neck squamous cell carcinoma

	PSCC (this study) (5 advanced tumors and 12 early tumors)						HNSC (TCGA) (497 tumors and 44 normal)		
miRNAs	Cytoband	Start-End (pb)	HPVis (genotype)*	miRNA Expression	Log2FC	*p-value*	miRNA Expression	Log2FC	*p-value*
miR-99a-5p	21q21.1	16,539,089-16,539,169	yes, (16, 18)	Upregulated	1.7381	0.0351	Downregulated	0.3	<0.0001
miR-150-5p	19q13.33	50,004,042-50,004,125	yes, (16)	Upregulated	1.4423	0.0324	Upregulated	1.08	0.21
miR-155-5p	21q21.3	26,946,292-26,946,356	yes, (16, 18)	Upregulated	1.3684	0.0264	Upregulated	1.56	0.0026
let-7c-5p	21q21.1	16,539,828-16,539,911	yes, (16, 18)	Upregulated	1.1359	0.0280	Downregulated	0.33	<0.0001
miR-342-3p	14q32.2	100,575,992-100,576,090	yes, (16, 18)	Upregulated	1.1259	0.0077	Upregulated	1.87	<0.0001
miR-891a-5p	Xq27.3	145,109,312-145,109,390	yes, (16)	Downregulated	-1.8318	0.0077	Downregulated	0.75	<0.0001
miR-376a-2-5p	14q32.31	101,040,069-101,040,148	yes, (16)	Downregulated	-1.8661	0.0054	Downregulated	0.61	0.044
miR-551b-3p	3q26.2	168,269,642-168,269,737	yes, (16)	Downregulated	-1.9444	0.0020	Upregulated	1.66	0.47
miR-1285-5p	7q21.2	91,833,329-91,833,412	yes, (16, 28, 31, 45)	Downregulated	-1.9779	0.0121	N/A	-	-
miR-362-3p	Xp11.23	49,773,572-49,773,636	yes, (16)	Downregulated	-2.6208	0.0091	Downregulated	0.65	<0.0001

*Data obtained from HPVBase [27] (accessed on April 12, 2022) and VISDB [28] we systematically collected and manually curated all VISs reported in the literature and publicly available data resources to construct the Viral Integration Site DataBase (VISDB), https://bioinfo.uth.edu/VISDB (https://bioinfo.uth.edu/VISDB/index.php/homepage) (accessed on April 12, 2022); miRNA = microRNA; HNSC = Head and Neck Squamous Cells Carcinoma; TCGA = The Cancer Genome Atlas; N/A = not available; HPVis = Human Papilloma Virus Integration Site.

and E7 oncoproteins in regulating networks of gene interactions and the ability of the virus to integrate into the human genome [27, 28]. In addition, we observed that 92% of the 25 miRDEs most altered (tumor *vs.* normal) are within HPVis, which supports that viral genome integration is one of the main mechanisms that lead to oncogene and miRNA dysregulation [27, 28, 31]. Additionally, we have also described genes and miRNAs present in genomic regions with CNAs that are also in HPVis [2, 7].

When performing a comparative analysis between miRDEs in hrHPV-PSCC and those differentially expressed in HNSC, we found that most miRDEs (80%, n = 20/25) had the same expression *status* in both tumors. This similarity of molecular profiles between HPV-associated squamous cell tumors grants the possibility of expanding the potential drugs to be tested in clinical trials given the rarity of penile tumors [32]. Furthermore, miR-1206 and miR-661, both downregulated in our samples, showed no changes in other cancers. The miR-1206 is one of six annotated miRNAs found at the non-coding PVT1 *locus* at 8q24 [33]. The role of miR-1206 is still unclear, although some evidence has shown that the PVT1 *locus* is linked to innate and adaptive immunity and p53 signaling functions [33]. In addition, some polymorphisms and variants have been described in miR-1206 in patients with acute lymphoblastic leukemia (ALL) and chronic myeloid leukemia (CML) being associated with methotrexate-induced oral mucositis and increased risk in CML [34, 35]. Ayoubian et al. [9] also identified this downregulated miRNA in HPV-positive penile tumors. Therefore, miR-1206 may have significant clinical value in HPV-penile cancer. However, more studies should be carried out to support this hypothesis.

Recent studies on miR-661 have yielded apparently conflicting conclusions, demonstrating that this miRNA has antagonistic functions depending on the type of cancer [36-39]. In glioma, miR-661 is often reported to be downregulated, inhibiting proliferation, migration, and invasion of tumor cells by regulating *hTERT* and participating in the regulation of competing for endogenous RNAs (ceRNAs) [37, 39]. In breast cancer, miR-661 can target *MDM2* and *MDM4* increasing p53 activity. However, depending on whether the p53 gene is wild-type or mutant, miR-661 can either inhibit or increase cancer aggressiveness [36]. On the other hand, in small-cell lung cancer, miR-661 promotes tumor invasion and metastasis by inhibiting *RB1* [38].

We identified 12 miRDEs associated with clinical and histopathological characteristics. MiR-1206, miR-376b-3p and miR-495-3p are downregulated miRNAs that are associated with perineural invasion. miR-376b-3p is a tumor suppressor that regulates proliferation, metastasis, and apoptosis by inhibiting *RGS1* [40]. Ayoubian et al. [9] reported that the sequence miR-376b-5p is downregulated in HPV-positive penile tumors. Our study is the first to our knowledge to demonstrate that antagomir (3p) is also downregulated in HPV-PSCC. MiR-495-3p is a tumor suppressor that inhibits cell proliferation, invasion, and migration via the modulation of the axis C1q/TNF-protein-related 3 [41] and regulates many epigenetic modifiers, including DNA-methyltransferase-1 (*DNMT1*) [42]. Interestingly, the HPV E7 oncoprotein binds to DNMT1 and enhances its DNA-methyltransferase activity. Furthermore, the HPV E7 oncoprotein can activate DNMT1 transcription via the pRB/E2F pathway [43]. These findings provide support that HPV can regulate the expression of genes and miRNAs through DNA methylation. Additionally, Barzon et al. [44] demonstrated that the tumor suppressor miR-218-1 is downregulated in HPV-penile tumors due to hypermethylation of the *SLIT2* promoter, which harbors *MIR218-1*.

The prediction of mRNA/miRDE interactions revealed genes that had not yet been described in penile cancer. *MDM2* (regulated by miR-661, which was found to be downregulated) and *MDM4* (regulated by miR-433-3p and miR-661, both of which were found to be downregulated) are responsible for negatively controlling p53 protein levels via ubiquitination and degradation [36]. Furthermore, the tumor suppressor *PTEN* was identified as the target of three upregulated miRNAs (miR-22-3p, miR-205-5p, and miR-130a-3p). In a previous investigation of the same cohort, a decrease in p53 protein expression (87.5%, n = 14/16 evaluated cases) and *TP53* mRNA (85.7%, n = 12/14 evaluated cases) was observed [2]. One of the possible mechanisms for this regulation is the activity of miRNAs, which we addressed in our previous

study [8]. We also demonstrated *PTEN* copy number loss and deletion (88.8%, n = 8/9 evaluated cases) [2]. In this present study, we provide evidence that epigenetic mechanisms can also downregulate *PTEN*.

The *in-silico* analysis of human-proteins *vs.* virus-proteins interactions showed important genes that can be regulated by HPV oncoproteins and by miRDEs. HPV proteins have the capacity to reprogram cellular signal transduction pathways [45]. In addition, the prediction of pharmacological targets showed inhibitors targeting *MDM2*, a target gene of downregulated miRNAs in PSCC. As the expression of these p53 inactivators is increased in several cancers, drugs to reactivate p53 has emerged as a promising therapeutic strategy for cancer [46]. Nutlin-3 is a cis-imidazoline that inhibits the interaction between MDM2 and p53, therefore inducing apoptosis. The nutlin-3 structure is also used as a model for developing several other compounds with the same function, some of which have an inhibitory effect superior to that of nutlin-3 [46].

The miRDEs analysis of two clinical groups (advanced and early diseases) revealed differential expression of 143 miRNAs, of which the top 10 miRDEs have high accuracy (AUC = 0.8) to discriminate the clinical groups. Two panels of miRDEs reached AUC = 0.9 (miR-99a-5p + miR-150-5p + miR-155-5p + let-7c-5p + miR-342-3p, all of them were found upregulated; and miR-376a-2-5p + miR-551b-3p, both found to be downregulated). Noteworthy that a single miRNA (miR-376a-2-5p) was able to discriminate between advanced and early diseases with high AUC score (0.9; P = 0.0114). To date, there are no studies on miR-376a-2-5p, and there is only one experimentally target described, *SRPK1* gene (Serine/Arginine-Rich Splicing Factor Kinase 1), which hybridizes by ligation of the type 7mer-m8 at position 1542-1563, 3'UTR (Untranslated region) (predicted by miRTarBase, PAR-CLIP/AGO2 data). Interestingly, all these 10 miRDEs are within HPVis, including HPV16 subtype, the most prevalent in the PSCC patients. We also highlight that all upregulated miRNAs (let-7c-5p, miR-150-5p, miR-155-5p, miR-342-3p, and miR-99a-5p) have been associated with resistance to anticancer drugs (doxorubicin, cisplatin, paclitaxel, gefitinib, and taxanes) [47-50]. Future studies with genetic targeting of these miRDEs may open new therapeutic opportunities in patients with hrHPV-PSCC.

In conclusion, the interaction networks involving HPV and miRNAs are highly complex and involve several micro and macro pathways. In this study, we provided PSCC molecular signature based on miRNAs differentially expressed. We showed that five miRNAs in hrHPV-PSCC and HNSC present similar expression status, opening the possibility of potential target drugs to be tested in both squamous cell carcinomas. We also described miRDEs regulating pathways involved in tumor development and associated to important clinical parameters such as perineural invasion, tumor grade, and staging. We highlight miR-376a-2-5p as a potential prognostic marker for hrHPV-associated PSCC patients. The small sample size is a limitation of this research, but based on our findings, future functional studies will be conducted to better understand the role of top miRNAs, and in particular the miR-376a-2-5p in this rare and severe tumor, thereby offering an opportunity for advances in diagnosis, prevention, and early therapy.

Acknowledgements

This research was supported by Fundação de Amparo à Pesquisa e ao Desenvolvimento Científico e Tecnológico do Maranhão (FAPEMA) - Grant number IECT-05551/18 and Uniscience - nanoString miRNA Grant for Silma Regina Pereira, and by Comissão de Aperfeiçoamento de Pessoal do Nível Superior (CAPES; code 001) for providing scholarship for Jenilson da Silva. André Alvares Marques Vale is a post-doctoral research fellow and scholarship holder of CAPES, grant number 88887.510243/2020-00 (PDPG Amazônia Legal). The APC was supported by FAPEMA/AGEUFMA EDITAL PRÓ-PUBLICAÇÃO Number 03/2023 and by CAPES (PDPG Consolidação 3-4; Number 88881.707439/2022-01).

Disclosure of conflict of interest

The authors declare that this research was conducted in the absence of any commercial or financial relationship that could be interpreted as a potential conflict of interest.

Address correspondence to: Silma Regina Pereira, Laboratory of Genetics and Molecular Biology, Department of Biology, Federal University of

Maranhão, São Luís 65080-805, MA, Brazil. Tel: +55-98-32728543; ORCID: 0000-0003-2974-3687; E-mail: silma.pereira@ufma.br

References

[1] Christodoulidou M, Sahdev V, Houssein S and Muneer A. Epidemiology of penile cancer. Curr Probl Cancer 2015; 39: 126-36.

[2] Macedo J, Silva E, Nogueira L, Coelho R, da Silva J, Dos Santos A, Teixeira-Júnior AA, Belfort M, Silva G, Khayat A, de Oliveira E, Dos Santos AP, Cavalli LR and Pereira SR. Genomic profiling reveals the pivotal role of hrHPV driving copy number and gene expression alterations, including mRNA downregulation of *TP53* and *RB1* in penile cancer. Mol Carcinog 2020; 59: 604-17.

[3] Hansen BT, Orumaa M, Lie AK, Brennhovd B and Nygård M. Trends in incidence, mortality and survival of penile squamous cell carcinoma in Norway 1956-2015. Int J Cancer 2018; 142: 1586-93.

[4] Protzel C, Alcaraz A, Horenblas S, Pizzocaro G, Zlotta A and Hakenberg OW. Lymphadenectomy in the surgical management of penile cancer. Eur Urol 2009; 55: 1075-88.

[5] Paner GP, Stadler WM, Hansel DE, Montironi R, Lin DW and Amin MB. Updates in the eighth edition of the tumor-node-metastasis staging classification for urologic cancers. Eur Urol 2018; 73: 560-569.

[6] Zhou X, Qi F, Zhou R, Wang S, Wang Y, Wang Y, Chen C, Wang Y, Yang J and Song W. The role of perineural invasion in penile cancer: a meta-analysis and systematic review. Biosci Rep 2018; 38: BSR20180333.

[7] Silva JD, Nogueira L, Coelho R, Deus A, Khayat A, Marchi R, Oliveira E, Santos APD, Cavalli L and Pereira S. HPV-associated penile cancer: impact of copy number alterations in miRNA/mRNA interactions and potential druggable targets. Cancer Biomark 2021; 32: 147-60.

[8] da Silva J, da Costa CC, de Farias Ramos I, Laus AC, Sussuchi L, Reis RM, Khayat AS, Cavalli LR and Pereira SR. Upregulated miRNAs on the TP53 and RB1 binding seedless regions in high-risk HPV-associated penile cancer. Front Genet 2022; 13: 875939.

[9] Ayoubian H, Heinzelmann J, Hölters S, Khalmurzaev O, Pryalukhin A, Loertzer P, Heinzelbecker J, Lohse S, Geppert C, Loertzer H, Wunderlich H, Bohle RM, Stöckle M, Matveev VB, Hartmann A and Junker K. miRNA expression characterizes histological subtypes and metastasis in penile squamous cell carcinoma. Cancers (Basel) 2021; 13: 1480.

[10] Furuya TK, Murta CB, Murillo Carrasco AG, Uno M, Sichero L, Villa LL, Cardilli L, Coelho RF, Guglielmetti GB, Cordeiro MD, Leite KRM, Nahas WC, Chammas R and Pontes J Jr. Disruption of miRNA-mRNA networks defines novel molecular signatures for penile carcinogenesis. Cancers (Basel) 2021; 13: 4745.

[11] Hartz JM, Engelmann D, Fürst K, Marquardt S, Spitschak A, Goody D, Protzel C, Hakenberg OW and Pützer BM. Integrated loss of miR-1/miR-101/miR-204 discriminates metastatic from nonmetastatic penile carcinomas and can predict patient outcome. J Urol 2016; 196: 570-8.

[12] Kuasne H, Barros-Filho MC, Busso-Lopes A, Marchi FA, Pinheiro M, Muñoz JJ, Scapulatempo-Neto C, Faria EF, Guimarães GC, Lopes A, Trindade-Filho JC, Domingues MA, Drigo SA and Rogatto SR. Integrative miRNA and mRNA analysis in penile carcinomas reveals markers and pathways with potential clinical impact. Oncotarget 2017; 8: 15294-306.

[13] Murta CB, Furuya TK, Carrasco AGM, Uno M, Sichero L, Villa LL, Faraj SF, Coelho RF, Guglielmetti GB, Cordeiro MD, Leite KRM, Nahas WC, Chammas R and Pontes J Jr. miRNA and mRNA expression profiles associated with lymph node metastasis and prognosis in penile carcinoma. Int J Mol Sci 2022; 23: 7103.

[14] Zhang L, Wei P, Shen X, Zhang Y, Xu B, Zhou J, Fan S, Hao Z, Shi H, Zhang X, Kong R, Xu L, Gao J, Zou D and Liang C. MicroRNA expression profile in penile cancer revealed by next-generation small RNA sequencing. PLoS One 2015; 10: e0131336.

[15] Moch H, Cubilla AL, Humphrey PA, Reuter VE and Ulbright TM. The 2016 WHO classification of tumours of the urinary system and male genital organs-part A: renal, penile, and testicular tumours. Eur Urol 2016; 70: 93-105.

[16] Hennig C. fpc: Flexible Procedures for Clustering. Fpc: Flexible Procedures for Clustering 2020. https://CRAN.R-project.org/package=fpc (accessed August 5, 2021).

[17] Cerami E, Gao J, Dogrusoz U, Gross BE, Sumer SO, Aksoy BA, Jacobsen A, Byrne CJ, Heuer ML, Larsson E, Antipin Y, Reva B, Goldberg AP, Sander C and Schultz N. The cBio cancer genomics portal: an open platform for exploring multidimensional cancer genomics data. Cancer Discov 2012; 2: 401-4.

[18] Gao J, Aksoy BA, Dogrusoz U, Dresdner G, Gross B, Sumer SO, Sun Y, Jacobsen A, Sinha R, Larsson E, Cerami E, Sander C and Schultz N. Integrative analysis of complex cancer genomics and clinical profiles using the cBioPortal. Sci Signal 2013; 6: pl1.

[19] Li JH, Liu S, Zhou H, Qu LH and Yang JH. starBase v2.0: decoding miRNA-ceRNA, miRNA-ncRNA and protein-RNA interaction networks

from large-scale CLIP-Seq data. Nucleic Acids Res 2014; 42: D92-7.
[20] Chandrashekar DS, Bashel B, Balasubramanya SAH, Creighton CJ, Ponce-Rodriguez I, Chakravarthi BVSK and Varambally S. UALCAN: a portal for facilitating tumor subgroup gene expression and survival analyses. Neoplasia 2017; 19: 649-58.
[21] Karagkouni D, Paraskevopoulou MD, Chatzopoulos S, Vlachos IS, Tastsoglou S, Kanellos I, Papadimitriou D, Kavakiotis I, Maniou S, Skoufos G, Vergoulis T, Dalamagas T and Hatzigeorgiou AG. DIANA-TarBase v8: a decade-long collection of experimentally supported miRNA-gene interactions. Nucleic Acids Res 2018; 46: D239-D245.
[22] Huang HY, Lin YC, Li J, Huang KY, Shrestha S, Hong HC, Tang Y, Chen YG, Jin CN, Yu Y, Xu JT, Li YM, Cai XX, Zhou ZY, Chen XH, Pei YY, Hu L, Su JJ, Cui SD, Wang F, Xie YY, Ding SY, Luo MF, Chou CH, Chang NW, Chen KW, Cheng YH, Wan XH, Hsu WL, Lee TY, Wei FX and Huang HD. miRTarBase 2020: updates to the experimentally validated microRNA-target interaction database. Nucleic Acids Res 2020; 48: D148-D154.
[23] Vlachos IS, Zagganas K, Paraskevopoulou MD, Georgakilas G, Karagkouni D, Vergoulis T, Dalamagas T and Hatzigeorgiou AG. DIANA-miRPath v3.0: deciphering microRNA function with experimental support. Nucleic Acids Res 2015; 43: W460-6.
[24] Kotlyar M, Pastrello C, Sheahan N and Jurisica I. Integrated interactions database: tissue-specific view of the human and model organism interactomes. Nucleic Acids Res 2016; 44: D536-41.
[25] Szklarczyk D, Gable AL, Lyon D, Junge A, Wyder S, Huerta-Cepas J, Simonovic M, Doncheva NT, Morris JH, Bork P, Jensen LJ and Mering CV. STRING v11: protein-protein association networks with increased coverage, supporting functional discovery in genome-wide experimental datasets. Nucleic Acids Res 2019; 47: D607-D613.
[26] Oughtred R, Rust J, Chang C, Breitkreutz BJ, Stark C, Willems A, Boucher L, Leung G, Kolas N, Zhang F, Dolma S, Coulombe-Huntington J, Chatr-Aryamontri A, Dolinski K and Tyers M. The BioGRID database: a comprehensive biomedical resource of curated protein, genetic, and chemical interactions. Protein Sci 2021; 30: 187-200.
[27] Kumar Gupta A and Kumar M. HPVbase -- a knowledgebase of viral integrations, methylation patterns and microRNAs aberrant expression: as potential biomarkers for Human papillomaviruses mediated carcinomas. Sci Rep 2015; 5: 12522.
[28] Tang D, Li B, Xu T, Hu R, Tan D, Song X, Jia P and Zhao Z. VISDB: a manually curated database of viral integration sites in the human genome. Nucleic Acids Res 2020; 48: D633-D641.
[29] Yang X, Yang S, Li Q, Wuchty S and Zhang Z. Prediction of human-virus protein-protein interactions through a sequence embedding-based machine learning method. Comput Struct Biotechnol J 2019; 18: 153-61.
[30] Freshour SL, Kiwala S, Cotto KC, Coffman AC, McMichael JF, Song JJ, Griffith M, Griffith OL and Wagner AH. Integration of the drug-gene interaction database (DGIdb 4.0) with open crowdsource efforts. Nucleic Acids Res 2021; 49: D1144-D1151.
[31] Tuna M and Amos CI. Next generation sequencing and its applications in HPV-associated cancers. Oncotarget 2017; 8: 8877-8889.
[32] Ghafouri-Fard S, Gholipour M, Taheri M and Shirvani Farsani Z. MicroRNA profile in the squamous cell carcinoma: prognostic and diagnostic roles. Heliyon 2020; 6: e05436.
[33] Bisio A, De Sanctis V, Del Vescovo V, Denti MA, Jegga AG, Inga A and Ciribilli Y. Identification of new p53 target microRNAs by bioinformatics and functional analysis. BMC Cancer 2013; 13: 552.
[34] Gutierrez-Camino A, Oosterom N, den Hoed MAH, Lopez-Lopez E, Martin-Guerrero I, Pluijm SMF, Pieters R, de Jonge R, Tissing WJE, Heil SG, García-Orad A and Van Den Heuvel-Eibrink MM. The miR-1206 microRNA variant is associated with methotrexate-induced oral mucositis in pediatric acute lymphoblastic leukemia. Pharmacogenet Genomics 2017; 27: 303-6.
[35] Hassan FM. The association of rs2114358 in the miR-1206 polymorphism to chronic myeloid leukemia. Microrna 2019; 8: 248-52.
[36] Hoffman Y, Bublik DR, Pilpel Y and Oren M. miR-661 downregulates both Mdm2 and Mdm4 to activate p53. Cell Death Differ 2014; 21: 302-9.
[37] Li Z, Liu YH, Diao HY, Ma J and Yao YL. MiR-661 inhibits glioma cell proliferation, migration and invasion by targeting hTERT. Biochem Biophys Res Commun 2015; 468: 870-6.
[38] Liu F, Cai Y, Rong X, Chen J, Zheng D, Chen L, Zhang J, Luo R, Zhao P and Ruan J. MiR-661 promotes tumor invasion and metastasis by directly inhibiting RB1 in non small cell lung cancer. Mol Cancer 2017; 16: 122.
[39] Liu Y, Yuan J, Zhang Q, Ren Z, Li G and Tian R. Circ_0016347 modulates proliferation, migration, invasion, cell cycle, and apoptosis of osteosarcoma cells *via* the miR-661/IL6R axis. Autoimmunity 2022; 55: 264-274.
[40] Zhang L, Yao M, Ma W, Jiang Y and Wang W. MicroRNA-376b-3p targets RGS1 mRNA to in-

hibit proliferation, metastasis, and apoptosis in osteosarcoma. Ann Transl Med 2021; 9: 1652.
[41] Zhao G, Zhang L, Qian D, Sun Y and Liu W. miR-495-3p inhibits the cell proliferation, invasion and migration of osteosarcoma by targeting C1q/TNF-related protein 3. Onco Targets Ther 2019; 12: 6133-43.
[42] Eun JW, Kim HS, Shen Q, Yang HD, Kim SY, Yoon JH, Park WS, Lee JY and Nam SW. MicroRNA-495-3p functions as a tumor suppressor by regulating multiple epigenetic modifiers in gastric carcinogenesis. J Pathol 2018; 244: 107-119.
[43] Burgers WA, Blanchon L, Pradhan S, de Launoit Y, Kouzarides T and Fuks F. Viral oncoproteins target the DNA methyltransferases. Oncogene 2007; 26: 1650-5.
[44] Barzon L, Cappellesso R, Peta E, Militello V, Sinigaglia A, Fassan M, Simonato F, Guzzardo V, Ventura L, Blandamura S, Gardiman M, Palù G and Fassina A. Profiling of expression of human papillomavirus-related cancer miRNAs in penile squamous cell carcinomas. Am J Pathol 2014; 184: 3376-83.
[45] Mesri EA, Feitelson MA and Munger K. Human viral oncogenesis: a cancer hallmarks analysis. Cell Host Microbe 2014; 15: 266-82.
[46] Ribeiro CJ, Amaral JD, Rodrigues CM, Moreira R and Santos MM. Synthesis and evaluation of spiroisoxazoline oxindoles as anticancer agents. Bioorg Med Chem 2014; 22: 577-84.
[47] Kazmierczak D, Jopek K, Sterzynska K, Nowicki M, Rucinski M and Januchowski R. The profile of microRNA expression and potential role in the regulation of drug-resistant genes in cisplatin- and paclitaxel-resistant ovarian cancer cell lines. Int J Mol Sci 2022; 23: 526.
[48] Saberinia A, Alinezhad A, Jafari F, Soltany S and Akhavan Sigari R. Oncogenic miRNAs and target therapies in colorectal cancer. Clin Chim Acta 2020; 508: 77-91.
[49] Zheng F, Zhang H and Lu J. Identification of potential microRNAs and their targets in promoting gefitinib resistance by integrative network analysis. J Thorac Dis 2019; 11: 5535-46.
[50] Chen D, Bao C, Zhao F, Yu H, Zhong G, Xu L and Yan S. Exploring specific miRNA-mRNA axes with relationship to taxanes-resistance in breast cancer. Front Oncol 2020; 10: 1397.

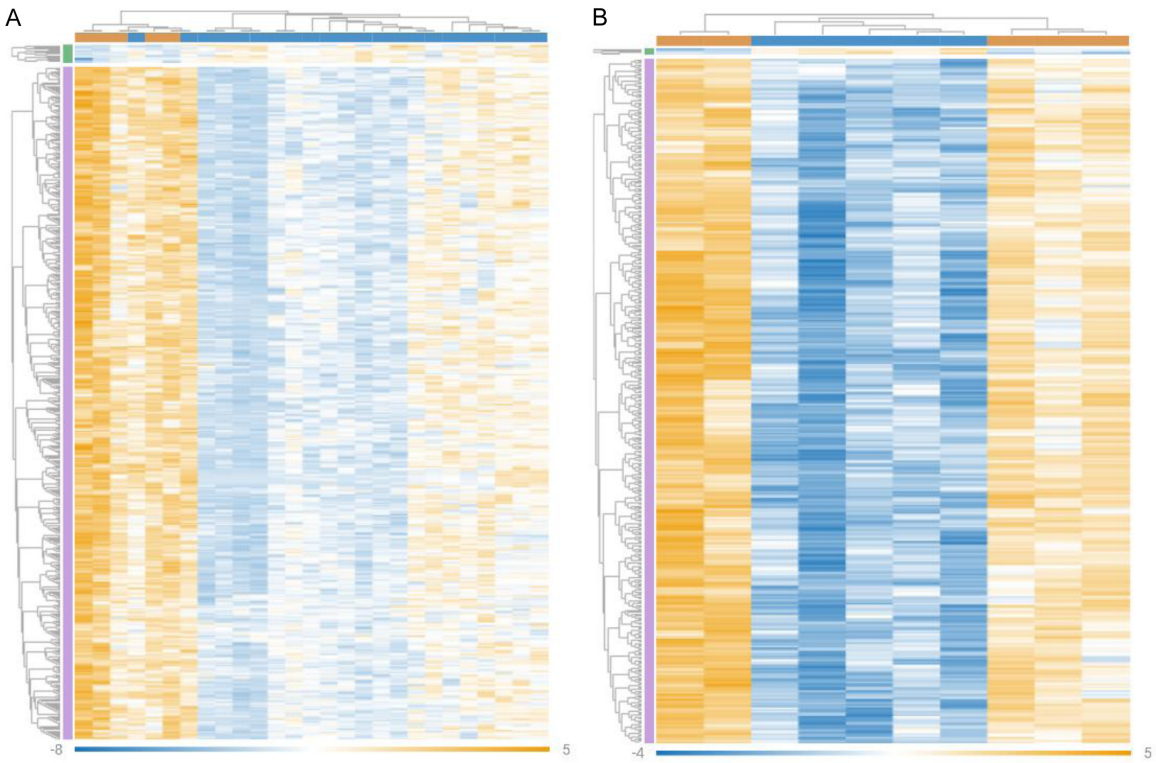

Supplementary Figure 1. The profile of differentially expressed miRNAs in all samples (A) and paired samples (B). In (A), the heatmap generated by the expression patterns of miRNAs in all samples (22 tumors and 5 non-tumors). In (B), the heatmap generated by the expression patterns of miRNAs in paired samples (5 tumors and 5 non-tumors). Both heatmap showed two distinct groups (upper cluster) formed by tumor samples (blue bar) and non-tumor samples (orange bar). The hierarchical group left is formed by the upregulated miRNAs (green bar) and downregulated (pink bar). In the heatmap, the yellow-orange colors indicate upregulated miRNAs, and the blue colors indicate downregulated miRNAs.

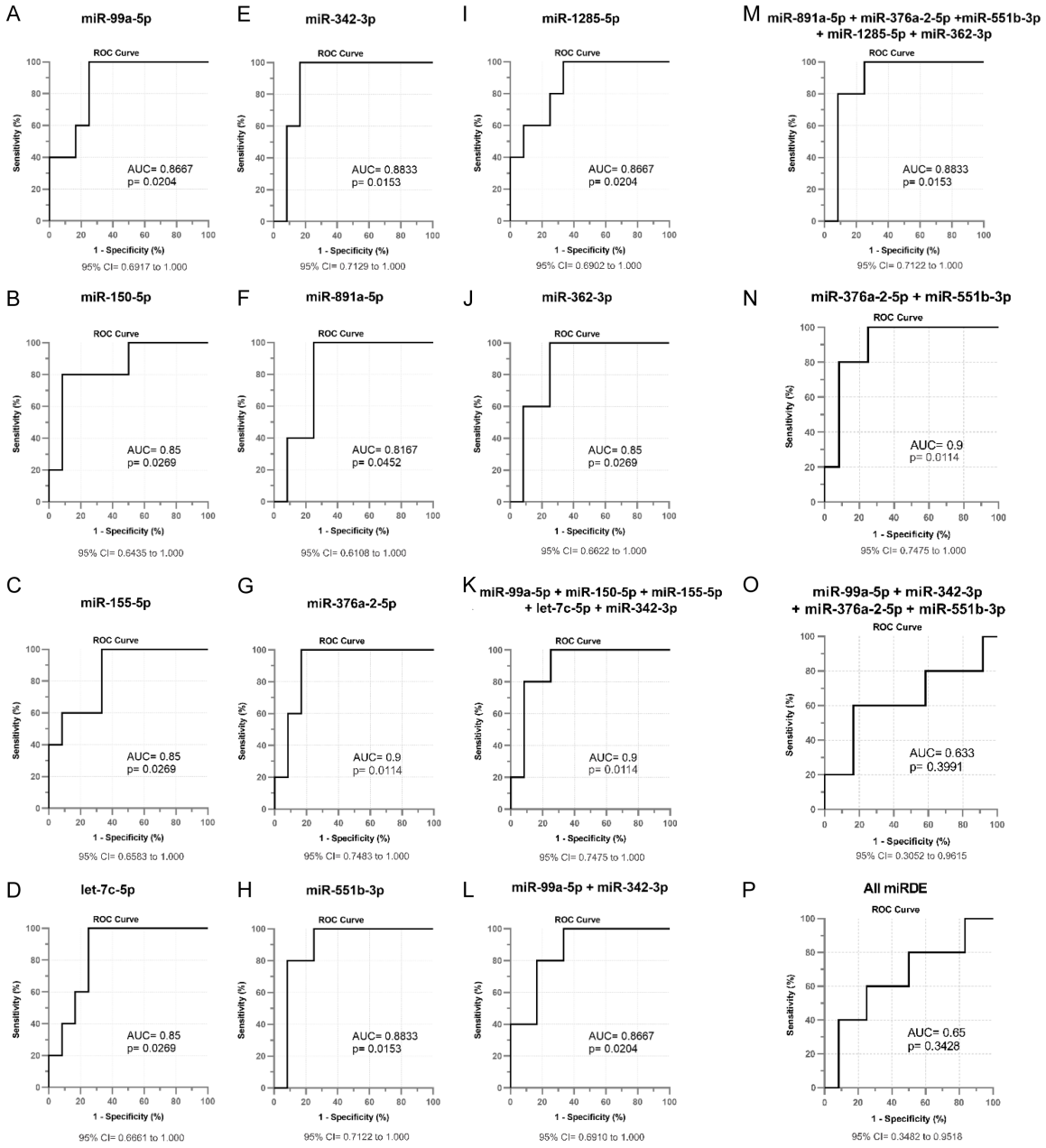

Supplementary Figure 2. ROC and AUC curve analysis of the top 10 miRDEs between clinical groups (advanced disease vs. early disease). A-P. ROC curve graphics showing AUC and *p*-values. On the -y axis is presented sensitivity versus 1-specificity on -x axis. Below each graph, the 95% CI value is presented.